Optimal design of piezo transducers with connected two-phase electrode

A. Donoso, E. Aranda

Departamento de Matemáticas,
ETSII, Universidad de Castilla-La Mancha,
Ciudad Real, Spain

D. Ruiz

Departamento de Matemáticas,
EIIA, Universidad de Castilla-La Mancha,
Toledo, Spain

Abstract

Tailor-made electrodes are of the utmost importance in the design of efficient piezoelectric transducers. Electrode patterns are given by polarization profiles which typically take on two values only, i.e. either positive or negative polarity. In general, optimized electrodes that enhance response of transducers exhibit isolated features of like-polarity; however, those lay-outs complicate wiring requirements as each feature must be connected to a current source. In this work, we adapt the method developed in [1] to ensure connectivity in topology optimization structures, which is based on known results of spectral graph theory, to design connected two-phase electrodes of easier manufacturability, still bearing in mind functionality.

Keywords: optimal design, piezo transducers, connectivity, two-phase electrode

1. Introduction

Piezoelectric transducers (actuators/sensors) are devices that convert mechanical energy into electrical energy, and vice versa, due to the reciprocity of the piezoelectric effect [2]. A quite common architecture of a piezoelectric

transducer is the one formed by a host structure sandwiched between two layers of piezoelectric materials, as depicted in Figure 1a. Depending on whether the piezo layers have been polarized in-phase or out-of-phase, the whole structure may undergo in-plane or out-of-plane displacements, respectively. The role of electrode in those structures is crucial as piezo materials are dielectric. That is the reason why an electrode on one of the sides of the piezo layers is required to collect the charge generated as a sensor to an external measurement device.

Typical electrode patterns correspond to polarization profiles which take on two values only, i.e. either positive or negative polarity. The fact of having two opposite polarities at our disposal is what allows to enhance considerably responses in piezo transducers. A good example of this is the electrode layout shown in Figure 1b. There, blue/red colors are areas of opposite polarity which mean that they are working in tension/compression. Otherwise, it would not have got the desired effect in the (in-plane) sensor on using only one polarity. Indeed, by shaping the electrode in an appropriate way, such devices can work as spatial filters in the frequency domain, what is also called modal transducers [3]. It means that they can measure (as sensors) or excite (as actuators) a single mode [4], or even a set of desired modes [5], whereas remaining insensitive to the rest of modes that belong to a bigger set. Figure 1c shows the electrode layout of a multimodal transducer that isolates both the first and the eleventh mode from the first (out-of-plane) twenty modes in a simply-supported plate. In this case, black/white non-connected phases denote areas of opposite polarity. Electrodes hardly ever present profiles of both phases connected as in Figure 1b. In general, the electrode layout is connected in one of the polarities at the best scenario, but it may not as in Figure 1c. In such cases, electrodes typically exhibit isolated features of like-polarity, which indeed makes it difficult the wiring schemes. In particular, the electrode profile in Figure 1c would require seven wires, as each feature must be connected to a current source. Moreover, the wiring must be done through the part of the boundary that is fixed.

In this work, we present a systematic procedure for designing connected two-phase electrodes, whose phases are in contact with the area where boundary

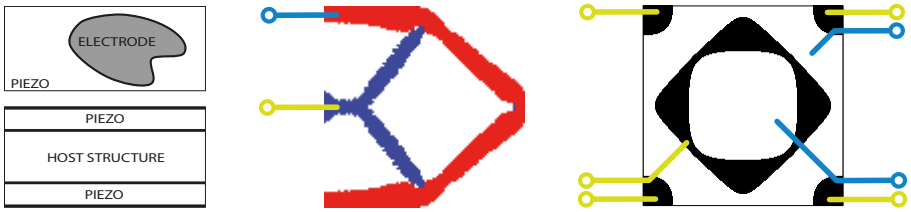

(a) (b) (c)

Figure 1: (a) Top and side views of the bimorph configuration of a piezoelectric structure. (b) Electrode layout (extracted from [6]) of a sensor fixed at its left side; blue/red connected phases are areas of opposite polarity, and white color means void (no host structure). (c) Electrode layout (extracted from [5]) of a multimodal transducer simply-supported at all four edges; black/white non-connected phases denote areas of opposite polarity.

conditions have been imposed. Electrode design problems can be formulated as optimization problems, where the surface electrode, which is a genuine 2d design domain, is discretized in finite elements, and a design variable taking any possible value between 0 (i.e. negative polarity) and 1 (i.e. positive polarity) is assigned to each finite element. The problem consists in determining which finite elements have positive polarity and which ones negative polarity for a given purpose. Although our proposal is valid in the context of piezoelectric transducers regardless of the objective function to be optimized, here we will focus on the case of modal transducers. This is because when designing modal (also multimodal) transducers [4, 5], optimal electrode profiles do not satisfy in general neither of the two aforementioned requirements.

Lack of connectivity is also an important issue in other physical contexts, particularly in structural design, where several enclosed holes usually appear in minimum compliance structures, leading to a distribution of the void phase that is not connected. Although it is desirable from a stiffness perspective, it complicates its manufacturing sometimes. In the last years, some authors have proposed different approaches ([7, 8, 9, 10, 11, 12, 13, 14]), some of them supported by physical arguments, to overcome that issue. In a very recent work [1], the authors developed a new method for addressing the structural

connectivity problem from a more mathematical perspective. It was called the algebraic connectivity method (ACM), and it is inspired by graph theory [15].

This work is aiming to generalize ACM in order to tackle the aforementioned electrode connectivity issue. It is a case of a genuine 2d scenario, where those two phases physically mean either positive or negative polarity of an electrode, but it may be extended to other contexts where coexisting two phases with another physical meaning.

The layout of the paper is as follows. Section 2 is dedicated to revising ACM and how it can be generalized for imposing connectivity in the two phases that coexist in the polarization profile. Section 3 is devoted to presenting a new formulation for designing modal transducers with connected two-phase electrode in the framework of a topology optimization problem. Section 4 provides some numerical examples that corroborate our approach. Finally, some conclusions and comments are provided in the last section.

2. The algebraic connectivity method (ACM) in electrode design

For a brief explanation of our method, let us consider the four coarse meshes 6×6 shown in Figure 2, where different (imaginary) electrode profiles of a modal piezo transducer fixed at its left side have been pictured. Each electrode is represented by a binary density where blue/red colors just denote areas with opposite polarity. These square meshes fully cover the design domain (i.e. the electrode) that we denote by Ω^I. To improve manufacturability of the electrode profiles and therefore obtain designs whose phases be also in contact with some part of the boundary conditions that is fixed (in this case, along the left edge), a small extension of Ω^I should be considered. It is important to notice that the location of the extensions physically represents the wiring positions for each phase. In these examples, we have taken as an extension just one finite element in the upper corner for the red phase (R), and another one in the lower conner for the blue phase (B). Each extra finite element along with the 6×6 mesh conform the two extended domains, hereafter denoted as $\Omega^E_X,\ X = R, B$. Next,

let us take a look to the connectivity issues in all four configurations.

Figure 2a is an example of electrode where the red phase is not connected in Ω^I, and the blue phase is not connected in Ω_B^E either, so it is not admissible. Electrode in Figure 2b is not admissible either, as the blue phase is still isolated from the extension. Figure 2c shows a configuration where the red phase is not connected in Ω_R^E, so it is again another example of a non-admissible profile. Finally, electrode in Figure 2d meets both requirements, as both phases are connected in Ω_B^E and in Ω_R^E, respectively. Note that this is the only case that requires only two wires, one for each phase.

Now, let us see how ACM is able to impose the connectivity requirements for this problem. Our method starts building two graphs associated to each phase of the initial domain, namely G_B^I for the blue phase and G_R^I for the red one. The nodes of each graph are the corresponding blue or red centroids of the finite elements in the mesh, respectively. Now we can characterize the connectivity of each phase by means of a well known result of graph theory [16]: *the number of connected components in a graph coincides with the multiplicity of the null eigenvalue in its Laplacian matrix*. In particular, for electrode profile in Figure 2a, the Laplacian matrix associated to graph G_R^I has two null eigenvalues, the first and the second, because they are two disconnected red areas. However the Laplacian matrix associated to G_B^I has a null eigenvalue only, as all blue phase is connected as a whole. Note however that graphs G_R^I and G_B^I corresponding to electrode profile in Figure 2b only have one null eigenvalue.

In order to move towards admissible configurations as the one depicted in Figure 2d, two additional graphs must be considered: the extended graphs G_B^E and G_R^E, which are the graphs that include the extension part as blue or red elements in each graph, respectively. The key point is that if the extension correspond to a really small portion on the boundary, the fact of forcing connectivity in the extended domains also ensures connectivity in the initial domain for both phases. Therefore, only two conditions are required for our purpose: G_B^E and G_R^E must be connected in Ω_B^E and Ω_R^E, respectively.

We will use eigenvalue problems for the Laplacian matrix of extended graphs

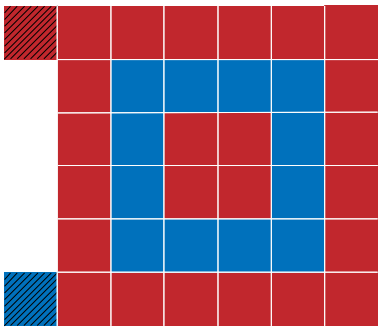

(a) Non-admissible electrode profile (red phase not connected in Ω^I; blue phase not connected in Ω_B^E).

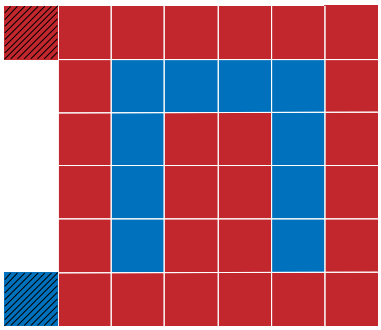

(b) Non-admissible electrode profile (blue phase not connected in Ω_B^E).

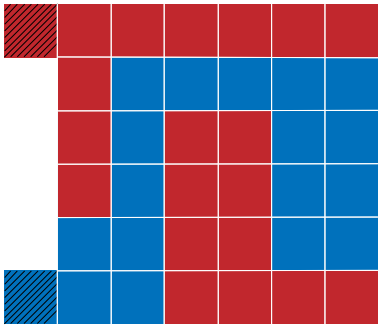

(c) Non-admissible electrode profile (red phase not connected in Ω_R^E).

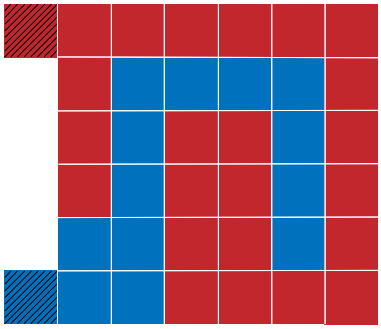

(d) Admissible electrode profile.

Figure 2: Finite electrode profiles for a transducer fixed at its left side; red/blue colors denote areas with opposite polarity in Ω^I; striped elements are the extensions, which represent the wiring positions for each phase. (a), (b) and (c) are non-admissible designs for the explained reasons into brackets in each situation, whereas (d) is admissible.

to impose connectivity constraints over the two phases. Therefore, it is imperative for our goal that the second smallest eigenvalue of the four Laplacian matrices be greater than zero. This invariant, called algebraic connectivity [16], gives a measure of how well connected an overall graph is, and here it puts partly a name to our method.

In all previous examples we have associated a graph to a structure defined by a binary density in a FE-mesh. In spite of the problem of modal transducers can be solved using linear programming and optimal electrode profiles have a binary structure [4], the introduction of connectivity constraints over the electrodes transforms this problem to nonlinear, making appear intermediate density values with no physical meaning in this case. Following the philosophy of the topology optimization method when using a density-based approach like SIMP [17] to solve this nonlinear problem, hereafter we will work with a density ρ that take continuous values in $[0, 1]$, where $\rho = 0$ means red polarity and $\rho = 1$ is blue polarity. This allows us to define two *weighted* graphs, each of them associated to each phase in Ω_X^E, and whose weights are defined as

$$(w_{ij})_R = (1 - \rho_i)(1 - \rho_j), \qquad (w_{ij})_B = \rho_i \rho_j, \tag{1}$$

where ρ_i and ρ_j are, respectively, the densities values at adjacent elements K_i, K_j of the mesh. If K_i and K_j are not adjacent, then $(w_{ij})_X = 0,\ X = R, B$.

The aforementioned result regarding graph connectivity for simple graphs [16] was also extended to weighted graphs with non-negative values on the edges [18], which lets us continue applying our same arguments with intermediate density values.

Note that, unlike the previous examples in which only elements belonging to a particular phase are considered as nodes for that graph, these new weighted graphs have as many nodes as elements in the mesh. So eventually, an entire row in the Laplacian matrix for the red phase could be null if the products $(1 - \rho_i)(1 - \rho_j) = 0$ for adjacent elements K_i and K_j, and $\rho_i \rho_j = 0$ in the Laplacian matrix for the blue phase. In that case, the number of null eigenvalues of Laplacian matrix would no longer reflects the number of connected components

of the void phase. We will introduce a parameter $W_{\min}$ to circumvent this effect.

On the other hand, a penalization of intermediate densities with a parameter q, in the same spirit as the SIMP does, is incorporated in (1) so the weights we are considering here are

$$(w_{ij})_R = ((1-\rho_i)(1-\rho_j))^q\,(1-W_{\min}) + W_{\min}, \tag{2}$$

and

$$(w_{ij})_B = (\rho_i\rho_j)^q\,(1-W_{\min}) + W_{\min}. \tag{3}$$

Therefore, the Laplacian matrix $\boldsymbol{\mathcal{L}}_X(\boldsymbol{\rho})$ may be obtained by assembling all elemental contributions between two adjacent nodes $i-j$, which are expressed as

$$(\boldsymbol{\mathcal{L}}_{i-j})_X = (w_{ij})_X \begin{pmatrix} 1 & -1 \\ -1 & 1 \end{pmatrix}.$$

After that, we build the matrix $\mathbf{M}_X(\boldsymbol{\rho}) \in \mathbb{R}^{n\times n}$ as the global (lumped) mass matrix that stores in its diagonal either the values $(1-\rho_i)|K_i|$ (in graph G_R^E) or the values $\rho_i|K_i|$ (in graph G_B^E), being $|K_i|$ the measure of the element K_i of the mesh, and n the number of nodes in the graph, that coincides with the number of the finite elements in the extended mesh.

To avoid some problems due to the null eigenvalue, it is convenient to apply a shifting in the eigenvalue problem, which leads to consider the following eigenvalue problem: find $((\lambda_m)_X, (\boldsymbol{\Phi}_m)_X)$ such that

$$\begin{aligned} (\boldsymbol{\mathcal{L}}_X(\boldsymbol{\rho}) - ((\lambda_m)_X - 1)\mathbf{M}_X(\boldsymbol{\rho}))(\boldsymbol{\Phi}_m)_X &= \mathbf{0}, \\ ((\boldsymbol{\Phi}_m)_X)^T\mathbf{M}_X(\boldsymbol{\rho})(\boldsymbol{\Phi}_m)_X &= 1, \end{aligned} \tag{4}$$

paying now attention to the multiplicity of the unit eigenvalue. Here, the pair $((\lambda_m)_X, (\boldsymbol{\Phi}_m)_X)$ corresponds to the eigenvalue and its associated $\mathbf{M}_X$-orthonormal eigenvector, respectively. In short, imposing connectivity over both phases in graphs G_X^E leads to forcing $(\lambda_2)_X > 1$ in the eigenproblem (4).

3. Problem formulation and sensitivity analysis

The problem of determining tailor-made electrodes to isolate a particular mode from a given set of modes can be formulated as a linear programing problem. We will not detail here nor the physics of the problem neither the problem formulation, and the reader is referred to [4] for comprehensive discussion, but we will give some interesting information about it. The most surprising fact is that not only does the problem admits optimal solutions, but also they are indeed unique [5], something that is not common at all to optimal design problems. Also there is a mathematical expression that lets characterize the electrode profiles in general, but it is far more practical to obtain them using linear programing over the discretized version of the problem.

As it was pointed out in the previous section, the incorporation of connectivity constraints over the electrodes transforms this problem to nonlinear. In our experience, this motivates us to formulate the optimal design problem by using a double-bound formulation with two extra non-negative variables, γ and α, which are the bounds added to the problem. That said, the discretized problem for isolating the k-th mode shape from a set of M modes ($j = 1, \cdots, M,\ j \neq k$) with connected two-phase electrode may be written

$$\max_{\gamma,\alpha,\boldsymbol{\rho}\in[0,1]} : (\gamma - \alpha)$$

subject to:

$$\begin{cases} \mathbf{G}_k^T(2\boldsymbol{\rho} - \mathbf{1}) \geq \gamma & \text{(to be isolated)} \\ |\mathbf{G}_j^T(2\boldsymbol{\rho} - \mathbf{1})| \leq \alpha & \text{(to be cancelled)} \\ \hline \tilde{\boldsymbol{\rho}} = \mathbf{H}(\boldsymbol{\rho}) & \text{(density filter)} \\ \hat{\boldsymbol{\rho}} = \mathbf{P}(\tilde{\boldsymbol{\rho}}) & \text{(0/1 projection)} \\ \left(\boldsymbol{\mathcal{L}}_X(\hat{\boldsymbol{\rho}}^\sharp) - ((\lambda_2)_X - 1)\mathbf{M}_X(\hat{\boldsymbol{\rho}}^\sharp)\right)(\boldsymbol{\Phi}_2)_X = \mathbf{0} & \text{(auxiliary eigenproblems)} \\ ((\boldsymbol{\Phi}_2)_X)^T\mathbf{M}_X(\hat{\boldsymbol{\rho}}^\sharp)(\boldsymbol{\Phi}_2)_X = 1 & (\mathbf{M}\text{-orthonormalization}) \\ (\lambda_2)_X > 1 & \text{(connectivity constraints)} \\ X = R, B \end{cases}$$

Here, $\mathbf{G}_j$ is a matrix related to the physics of the problem and, in particular, regarding the j-th mode shape. The role of γ and α that have been previously normalized so that they are always lower than 1, is to force the response of the k-th mode to stay over γ, whereas the response of the other modes is reduced to be below α; $\tilde{\boldsymbol{\rho}}$ is the filtered density; $\hat{\boldsymbol{\rho}}$ is the projected (filtered) density; and $\hat{\boldsymbol{\rho}}^{\sharp}$ corresponds to the extension of $\hat{\boldsymbol{\rho}}$ to the extended domain with 0/1 values, depending on whether we are dealing with red or blue phase.

Here, the filtered density at element K_e is defined by

$$\tilde{\rho}_e = \frac{\sum_i d_e(\mathbf{x}_i)\rho_i}{\sum_i d_e(\mathbf{x}_i)},$$

where $\mathbf{x}_i$ is the barycenter of element K_i, and the weighting function $d_e(\mathbf{x}_i)$ is given by the cone-shape function

$$d_e(\mathbf{x}_i) = \max\{r - \|\mathbf{x}_i - \mathbf{x}_e\|, 0\}.$$

where r is the filter radius. Unlike what happens in structural design, prescribed values of r do not seem to control minimum feature sizes of none of the phases, judging by numerical experiments. However, the use of this density filter ([19, 20]) lets regularize above finite-dimensional problem, favoring convergence on working with intermediate densities. But, on the contrary, this also produces some gray areas in the final layouts, and a thresholding projection method is then required to obtain closer 0/1 solutions. Here it is performed using a continuation method with the smoothed Heaviside function proposed in [21]

$$\hat{\rho}_e \equiv P(\tilde{\rho}_e; \beta, \eta) = \frac{\tanh(\beta\eta) + \tanh(\beta(\tilde{\rho}_e - \eta))}{\tanh(\beta\eta) + \tanh(\beta(1 - \eta))},$$

where $\hat{\rho}_e$ is the projected density of element K_e, the parameter β determines the sharpness of the projection and $\eta \in [0, 1]$ is the threshold parameter. All densities whose value is lower than η are approximate to 0, and the ones whose value is bigger than this parameter are approximate to 1. The specific values of these parameters will be mentioned at section 4.

With regard to the sensitivity analysis, we simply should carefully computing eigenvalues derivatives depending on whether eigenvalues are single or repeated, something that is well-known. The reader is referred to [1], that entirely contains all details about that issue. Once all the derivatives have been computed, the discretized problem is numerically solved by MMA [22], a non-linear programing solver that has been widely used and it continues to do so in structural optimization problems.

4. Numerical examples

This section is devoted to showing some numerical examples of connected two-phase electrodes obtained by ACM. Some of the followed strategies are the same in all examples and they are mentioned next. Regarding connectivity constraints, the condition $(\lambda_2)_X > 1$ is treated here as $(\lambda_2)_X \geq \lambda_2^{\min}$, where the value of the parameter $\lambda_2^{\min}$ has been chosen, from experience, around 1.15 to impose connectivity over both phases. Indeed, a continuation method has been implemented, beginning with $(\lambda_2)_X > 1.05$ and ending with $(\lambda_2)_X > 1.15$, increasing the value of the eigenvalue in 0.01 each 50 iterations. Concerning projection parameters, $\eta = 0.5$ and β is gradually increased from 2 to 64 at every 50 iterations, beginning when the iterative process starts to stabilize, which means approximately after 400 iterations.

We first consider a plate-type transducer fixed at its left edge. We are interesting in designing the electrode profile that maximizes the second mode shape only. This situation has been simulated by removing the bound α and its corresponding constraints from the problem formulation. The mesh used has 200×200 elements and the filter radius is $r = 8$ which corresponds to a filter size of 8 elements in any direction. In this case, we have fixed the upper square of 5×5 elements with density equal to 0 when imposing connectivity over red phase in Ω_R^E, and the lower square of 5×5 elements taking values equal to 1 when doing the same over blue phase in Ω_B^E. In the absence of connectivity constraints, the electrode profile required for such situation is a (2×2) checkerboard-type

distribution as Figure 3a shows. When imposing connectivity constrains, and depending on the starting point, the (new) admissible configurations Figure 3b or Figure 3c are obtained. Both of them depict really intuitive designs that require just two wires. And, what is more, the portion of each phase in contact with the boundary that is fixed gives us all allowed (equally valid) wiring locations. In practice, the new electrodes are just 5% worse than the one in Figure 3a, which indicates that they are indeed functional designs.

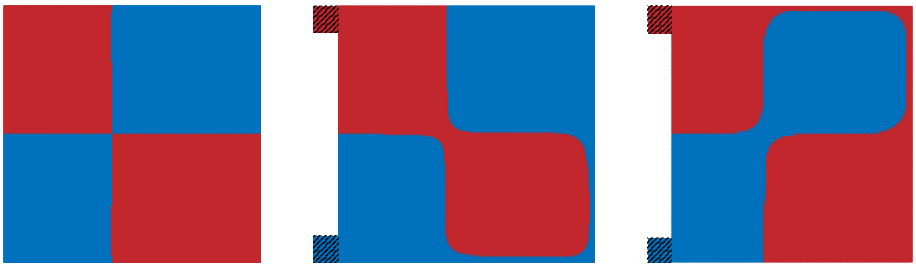

(a) (b) (c)

Figure 3: Electrode profiles that maximize the second mode shape in a plate fixed at its left edge; (a) without connectivity constraints; (b) and (c) with connectivity constraints corresponding to different starting points.

In our second example the plate is fixed at all four edges. Optimal electrode that maximizes the first mode and simultaneously cancels the influence of both second and third mode is depicted in Figure 4a for a mesh of 200×200. For the prescribed wiring positions showed in Figure 4b and Figure 4c and $r = 16$, electrode profiles exhibit the topologies that one would expect. Also, in terms of filtering efficiency, both of them are really good designs as $\gamma \approx 0.97$ and $\alpha = 2 \times 10^{-8}$.

The third case study is again a plate-type structure but now fixed at its left and right edges. This example was already treated under connectivity constraints in [23] using the virtual temperature method. The electrode profile that isolates the first mode from the fourteen out-of-plane modes is showed in Fig. 5a, with a configuration that would require four wires. Here, we have used again a mesh of 272×80 elements for this example, and $r = 8$. Considering the same

(a) (b) (c)

Figure 4: Electrode profiles that maximize the first mode shape from the first three out-of-plane modes in a plate fixed at all four edges; (a) without connectivity constraints; (b) and (c) with connectivity constraints corresponding to different prescribed wiring positions.

extensions as in the previous example, which correspond to different prescribed wiring locations, new electrode profiles meet all connectivity requirements. And both of them become excellent designs since $\gamma \approx 0.93$ and $\alpha = 1.5 \times 10^{-7}$ in Figure 5b, and $\gamma \approx 0.9$ and $\alpha = 1.5 \times 10^{-8}$ in Figure 5c.

Common to all optimized electrode profiles is the fact that they show really intuitive configurations, since in most cases they correspond to the designs that one would implement by imposing connectivity constraints a posteriori. However, our method lets us successfully introduce such constraints in the problem formulation rather than doing it at a later stage. In a future work we will focus on controlling the minimum feature size of the different phases involved in the problem, as in some parts they are about the size of the finite elements in the mesh.

5. Conclusions

This work provides a systematic procedure to impose connectivity constraints in the two polarity phases that typically appear in the electrodes of piezoelectric transducers. This technique, which is graph theory inspired, is a generalization of a method developed by the authors to avoid the formation of enclosed holes in topology optimized structures. It is worth highlighting that

(a)

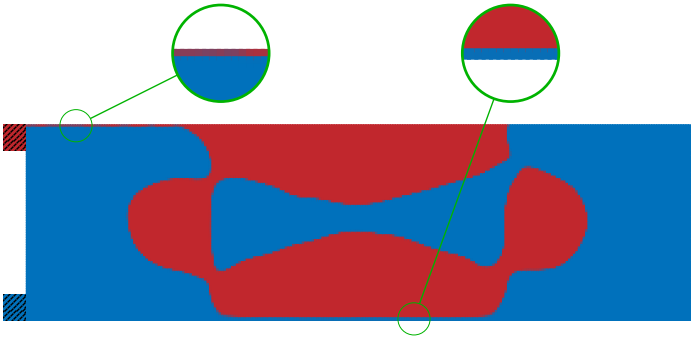

(b)

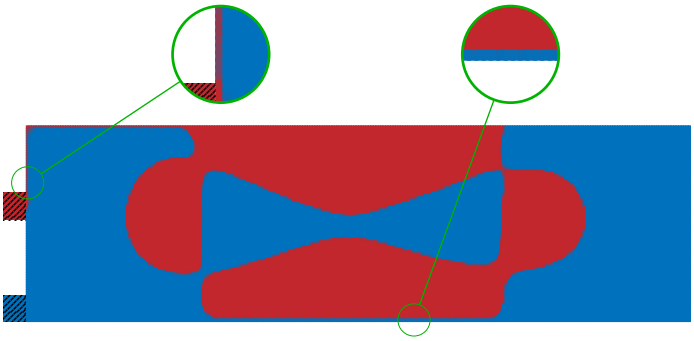

(c)

Figure 5: Electrode profiles that isolate the first mode from the first 14 out-of-plane modes in a plate fixed at both left and right edges; (a) without connectivity constraints; (b) and (c) with connectivity constraints corresponding to different prescribed wiring positions. Details of fine connections are shown.

our method allows to perform electrode design regardless the objection function and constraints of the problem in which the piezo transducer is involved. Selected examples come from the context of modal transducers, as electrode configurations are prone to exhibit isolated features of like-polarity. Judging by the numerical results, the new admissible electrodes are good samples of trade-off between functionality and manufacturability.

Acknowledgements Authors acknowledge financial support from the Spanish Ministerio de Ciencia e Innovación through grant PID2020-116207GB-I00, Junta de Castilla - La Mancha through grant SBPLY/19/180501/000110, and European Regional Development Fund 2018/11744.

References

[1] A. Donoso, E. Aranda, D. Ruiz, A new approach based on spectral graph theory to avoiding enclosed holes in topology optimization, Comput Methods Appl Mech Engrg (submitted).

[2] S. O. Moheimani, A. J. Fleming, Piezoelectric Transducers for Vibration Control and Damping, 2nd Edition, Springer, 2006.

[3] C. K. Lee, F. C. Moon, Modal sensors/actuators, J Appl Mech 57 (2) (1990) 434–441.

[4] A. Donoso, J. C. Bellido, Systematic design of distributed piezoelectric modal sensors/actuators for rectangular plates by optimizing the polarization profile, Struct Multidisc Optim 38 (4) (2009) 347–356.

[5] A. Donoso, J. C. Bellido, Robust design of multimodal piezoelectric transducers, Comput Methods Appl Mech Engrg 338 (2018) 27–40.

[6] D. Ruiz, J. Bellido, A. Donoso, J. Sánchez-Rojas, Design of in-plane piezoelectric sensors for static response by simultaneously optimizing the host structure and the electrode profile, Struct Multidisc Optim 48 (2013) 1023–1026.

[7] S. Liu, Q. Li, W. Chen, L. Tong, G. Cheng, An identification method for enclosed voids restriction in manufacturability design for additive manufacturing structures, Front Mech Eng 10 (2) (2015) 126–137.

[8] M. Osanov, J. Carstensen, E. Tromme, J. Guest, C. Williams, Topology optimization for additive manufacturing: New projection-based design algorithms, in: Proceedings of 17th AIAA/ISSMO Multidisciplinary Analysis and Optimization Conference, Aviation 2016, AIAA, Washington D.C., 2016, pp. 1–9.

[9] L. Zhou, W. Zhang, Topology optimization method with elimination of enclosed voids, Struct Multidisc Optim 60 (2019) 117–136.

[10] Y. Luo, O. Sigmund, Q. Li, S. Liu, Additive manufacturing oriented topology optimization of structures with self-supported enclosed voids, Computer Methods in Applied Mechanics and Engineering 372 (2020) 113385.

[11] C. Wang, B. Xu, Q. Meng, J. Rong, Y. Zhao, Numerical performance of poisson method for restricting enclosed voids in topology optimization, Computers & Structures 239 (2020) 106337.

[12] A. T. Gaynor, T. E. Johnson, Eliminating occluded voids in additive manufacturing design via a projection-based topology optimization scheme, Additive Manufacturing 33 (2020) 101149.

[13] G. Sabiston, I. Kim, Void region restriction for additive manufacturing via a diffusion physics approach, Int J Numer Methods Eng 121 (2020) 4347–4373.

[14] Y. Xiong, S. Yao, Z.-L. Zhao, Y. M. Xie, A new approach to eliminating enclosed voids in topology optimization for additive manufacturing, Additive Manufacturing 32 (2020) 101006.

[15] F. R. K. Chung, Spectral Graph Theory, American Mathematical Society, 1997.

[16] M. Fiedler, Algebraic connectivity of graphs, Czechoslovak Mathematical Journal 23 (2) (1973) 298–305.

[17] M. P. Bendsøe, O. Sigmund, Topology optimization: theory, methods, and applications, 2nd Edition, Springer, 2003.

[18] M. Fiedler, Laplacian of graphs and algebraic connectivity, Combinatorics and Graph Theory 25 (1989) 57–70.

[19] B. Bourdin, Filters in topology optimization, Int J Number Meth Engng 50 (9) (2001) 2143–2158.

[20] T. E. Bruns, D. A. Tortorelli, Topology optimization of nonlinear elastic structures and compliant mechanisms, Comput Methods Appl Mech Engrg 190 (26—27) (2001) 3443–3459.

[21] F. Wang, B. S. Lazarov, O. Sigmund, On projection methods, convergence and robust formulations in topology optimization, Struct Multidisc Optim 43 (6) (2011) 767–784.

[22] K. Svanberg, The method of moving asymptotes-a new method for structural optimization, Int J Number Meth Engng 24 (2) (1987) 359–373.

[23] A. Donoso, J. K. Guest, Topology optimization of piezo modal transducers considering electrode connectivity constraints, Computer Methods in Applied Mechanics and Engineering 356 (2019) 101–115.